CENTRIFUGAL COMPRESSOR TEST FACILITY WITH ACTIVE MAGNETIC BEARINGS

Eric S. Buskirk, Dorsa Sanadgol, Eric H. Maslen
University of Virginia, ROMAC Laboratories,
Department of Mechanical and Aerospace Engineering
Charlottesville, VA 22904, USA
esb3z@virginia.edu

Nathan K. Brown
Waukesha Magnetic Bearings
Franklin, CT 06254, USA
NBrown@us.waukbearing.com

ABSTRACT

Design of a test facility for assessing wheel loading of a centrifugal compressor is described. The facility uses active radial and axial magnetic bearings to estimate static and dynamic bearing loadings. The central application of the facility is to measure the loading forces on the impeller at non-design conditions. This data is then used to verify and refine analytical models for use in compressor design. In addition, the axial active magnetic bearing provides substantial control authority over the impeller tip-clearance, creating strong potential for active suppression of surge.

INTRODUCTION

The test facility presented in this paper analyzes an unshrouded centrifugal compressor. Pressures, temperatures and force loads on the impeller are all captured for off-design conditions. Active magnetic bearings (AMBs) will be used for both physical supports and force measure instruments. Being inherently contact-free and able to measure dynamic forces accurately, AMBs are an obvious candidate for this type of experimental testing.

Many, including Knopf et al.[1], Guinzburg et al.[2] and Baun et al.[3] have used AMBs to measure dynamic forces to test pumps, fluid-film bearings, compressors and other rotating machinery. Nordmann et al.[4] have presented extensive work on force measurement accuracy of AMBs: this work is examined later in the force measurement section of this paper. This test facility will use two radial and one axial AMB to properly constrain its movement and measure reaction forces at the bearing location.

Previous research by Spakovsky [5] used a radial AMB to manipulate the radial tip clearance of an axial compressor to suppress compressor surge. This test facility additionally will examine actuation of the axial AMB, changing the compressor tip-clearance, to suppress surge in the centrifugal compressor. The advantage of our research on surge control over Spakovsky's method is the ability to modulate the mean tip clearance of a centrifugal compressor instead of circumferentially modulating the tip clearance of an axial compressor.

Presented first is the design of the test facility with its five main sections: motor, test spindle, magnetic bearings, compressor and magnetic bearing controller. Emphasis is placed on the design of spindle, magnetic bearings and controller. Design criteria such as material selection, sensor placement and thermal cooling issues are presented as an aid to future design of similar apparatuses.

The rotor is levitated on active magnetic bearings. The AMBs' design and performance estimates are described, including a method of modelling and extending the bandwidth of the thrust bearing. An analytical evaluation of the thrust bearing's performance with high and low limits of the bandwidth are analyzed. The AMB controller with performance capability is also discussed. Finally, the method of force estimation is explained with realistic predictions of force measurement accuracy.

TEST FACILITY

This test facility has four main sections as shown in Figure 1. The motor provides the driving power; the coupling connects the motor to the testing section; the test section houses the magnetic bearings along with other instrumentation and the compressor is the device being

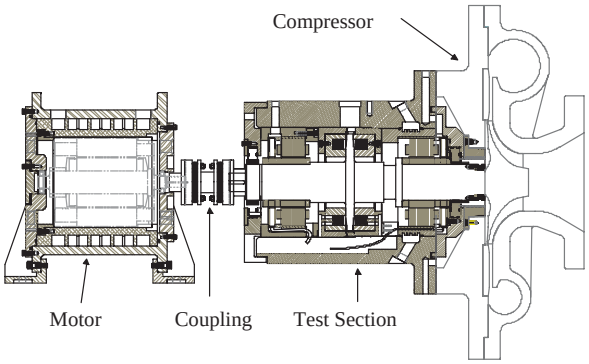

Figure 1: Assembly of Compressor Test Facility

tested. Each component is bolted to a rigid baseplate to ensure no vibration and consistent alignment.

Motor

The motor is a prototype induction motor produced by KaVo. Rated at 125kW at 30,000rpm and driven by a precision variable frequency drive, the motor has sufficient capacity to explore the compressor's entire range. At the compressor's design speed of 23,000rpm, the motor can produce up to 95kW of power. With the compressor rated at approximately 55kW, the motor can easily supply enough power to cover any loses including mechanical losses, impeller losses and bearing losses. The frequency drive is operated through a 0-10V control with National Instruments' LabView™. For safety, a separate control room is located roughly 30m(100ft) from the testing facility. A simple point-to-point calibration with a key phaser provides accurate speed control of the motor.

Since the motor is a prototype, there is no manufacturer's data for the thermal output of the motor. A water jacket surrounding the motor is part of a closed loop system with a forced convection radiator to remove excess heat. A thermal-resistance model of the motor's components was developed to assist in sizing the cooling system. The thermal model estimates the required heat dissipation to be 15kW and a peak temperature in the motor windings of 120°C(250°F).

Coupling

A Thomas 71 series coupling provides the connection between the motor spindle and the testing spindle. The flexible disk-pack coupling allows for sufficient axial and radial misalignment between the motor spindle (on hard bearings) and the testing spindle (on magnetic bearings). With the known axial stiffness and a maximum axial displacement of $\pm$0.51mm(0.020in) which is 50% of the thrust AMB nominal air gap, the coupling is expected to generate less than 65N(15lb) of axial force. Parallel misalignment between the motor spindle and testing

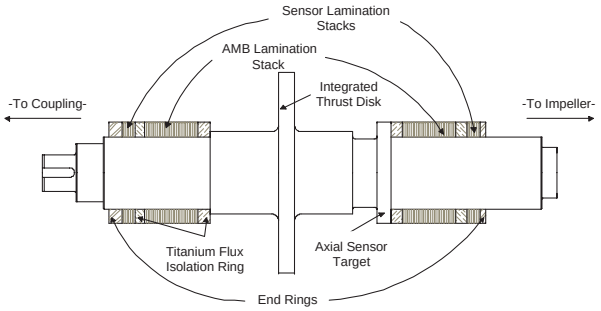

Figure 2: Testing Spindle with Lamination Stacks

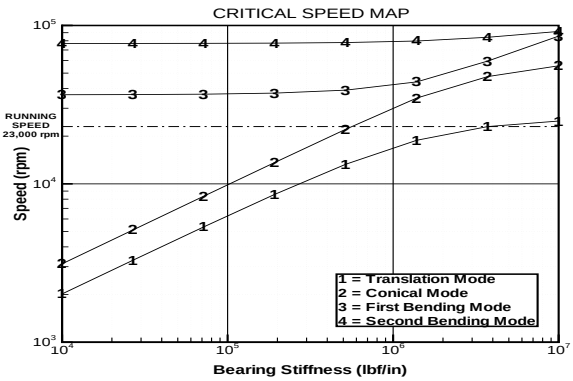

Figure 3: Critical Speed Map

spindle can reach 0.25mm(0.010in) with this coupling. This misalignment allows for wheel orbits on the order of 50% of the nominal clearances in the AMBs. Calibration will yield the radial stiffness of the coupling. With the known stiffness, the effects of the motor and flexible coupling can be removed from the force measurements of the compressor's impeller.

Test Section

The test section contains the main measurement instrumentation of the testing facility. Three AMBs provide both support and force measurement of the rigid test spindle.

Test Spindle

The spindle of the testing section is designed as a rigid rotor. Because of high running speed and an integrated magnetic thrust disk on the spindle, as shown in Figure 2, material selection is important for this element. ANSI 4340 steel was selected since it exhibits both high yield strength and acceptable magnetic properties.

The first critical bending mode of the spindle, designated with a 3 in Figure 3, occurs above 36,000rpm, more than 50% above the operating speed of the machine. A mode shape plot, Figure 4, was also created

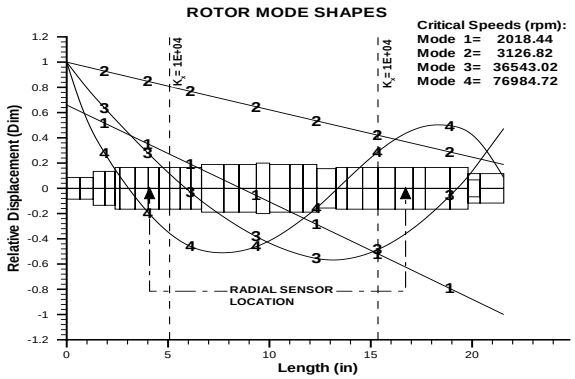

Figure 4: Mode Shape Plot

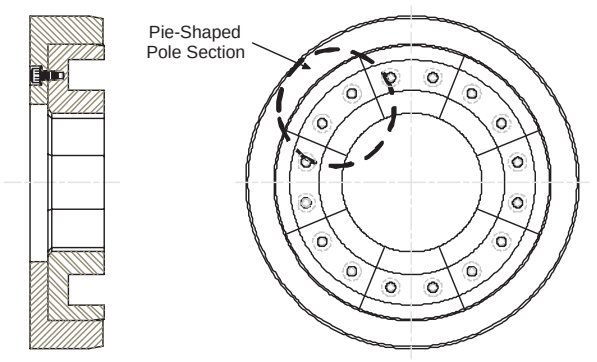

Figure 5: Magnetic Thrust Bearing: pie sections to reduce eddy currents.

to ensure the nodes of the bending modes did not occur at the radial position sensor locations. Both plots show good actuator control authority for the first and second bending modes.

Radial AMB

The two radial bearings are E-core in design. Each bearing is rated for a quadrant load capacity of 1400N (315lb) at the design flux density of 1.25T. Copley Controls Model 423 DC servo amplifiers are used to drive the magnetic bearings. These 25kHz switching amplifiers can provide a maximum continuous current of 15A at $\pm$170V and a maximum peak current of 30A at $\pm$170V. The amplifier's bandwidth in current mode is 3kHz. Coupling the amplifiers to the radial bearings, a slew rate for opposing quadrants of 4.3×10^6N/sec(9.7×10^5 lbf/sec) can be achieved with a 7A bias current. The rotor lamination stacks for the AMBs, shown in Figure 2, were made from bonded 0.127mm (0.005in) thickness silicon iron to reduce the eddy current effects.

Variable reluctance sensors aligned with each radial AMB axis provide accurate position measurements of the spindle for the controller. The target for each radial sensor is a separate lamination stack of 0.127mm (0.005in) silicon steel. Using a lamination stack as the target (instead of the bare shaft) is required because of the lower sensor frequencies (relative to eddy current sensors) and improves sensitivity by reducing any eddy current production in the target. Figure 2 shows a non-magnetic, titanium ring between the AMB lamination stack and the sensor target lamination stack. Its purpose is to isolate the magnetic flux in the AMB stack from the sensor lamination stack. Titanium had to be used instead of conventional materials like aluminum or stainless steel because of the high surface speed of the spindle. A centrifugal stress model showed that the high strength and low density of titanium were needed to maintain an appropriate shrink fit at both running speed and at rest.

Thrust AMB

The magnetic thrust bearing is an integral part of this test facility. Kobe Steel, the impeller manufacturer, predicted an impeller thrust loading of 3300N(740lbf); therefore, a double-acting magnetic thrust bearing was designed with a load capacity of 6600N(1480lbf), providing a factor of safety of 2. With a nominal air gap of 1.0mm(0.040in) on each side, the thrust bearing provides adequate clearance for actuating the tip-clearance of the impeller. For design, a worst-case air gap of 1.3mm(0.050in) is used to ensure adequate load capacity at any position. This worst-case is the 1.0mm(0.040in) nominal air gap displaced 0.25mm(0.010in). A magnetic thrust disk is monolithically fabricated on the test spindle made of ANSI 4340 steel, thus dictating a lower design flux of 1.2T. The axial magnetic thrust bearings along with the Copley amplifiers described earlier can achieve a slew rate of 1.3×10^6N/sec(2.8×10^5lbf/sec).

The bandwidth of the thrust actuator is very important since one objective of the test facility is to examine surge suppression by actuating the magnetic thrust bearing as described by Sanadgol et al.[6]. In order to reduce eddy current losses and improve actuator bandwidth, each pole face was cut into 8 separate pie-shaped sections that were later electrically insulated before reassembly. Each pole section is bolted to a non-magnetic retaining ring for support. Figure 5 shows the details of this design.

Performance estimates, Figure 6, of the thrust bearing were computed by Zhu et al.[7], [8]. Cut-off frequencies (-3dB from the DC response) were determined to be between 5.8 Hz and 135 Hz. The lower limit (solid line) of the performance was estimated using a solid thrust actuator model – this assumes that losses in the rotor dominate actuator performance. The upper limit (dashed line) attempted to study the effect of the pole sectioning by simulating the thrust bearing as eight separate C-cores – this assumes that losses in the stator dominate actuator performance. The actual thrust bearing performance should

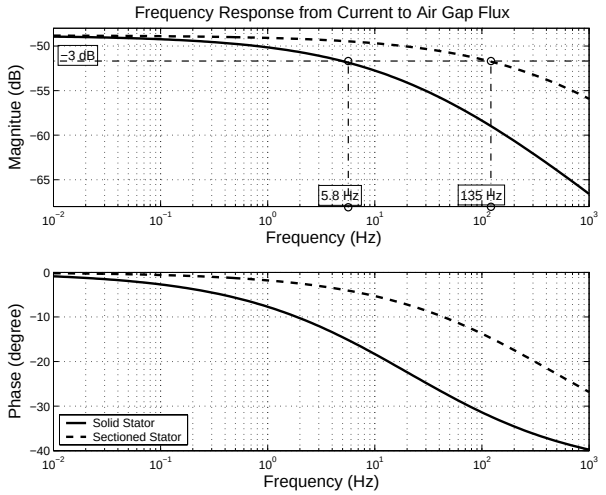

Figure 6: Thrust bearing bandwidth predictions.

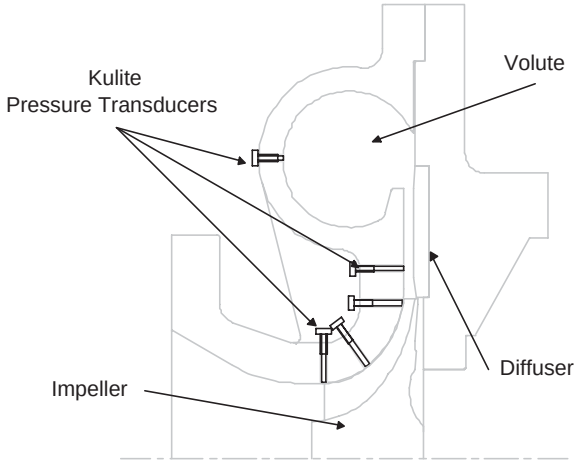

Figure 7: Pressure Sensor Placement

lie between the two curves and, given the relatively large volume of stator iron in comparison to rotor iron, we are optimistic of realizing a relatively high bandwidth: on the order of 85 Hz.

Axial position measurement is performed with two SKF 5mm(0.20in) button eddy current probes. Both probes target a shoulder on the spindle as shown in Figure 2. The shoulder target was placed between the thrust disk and impeller location. Since the impeller end of the spindle will get substantially hotter than the opposing end, thermal expansion when the test rig is running can cause substantial error between the axial position of the shaft and the axial tip–clearance of the impeller. Placing the sensor target close to the impeller will reduce this error and still provide a good measurement of the thrust bearing air gap.

Backup Bushings

To ensure no metal–to–metal contact, two auxiliary bushings were installed in the test facility. Cut from oil–impregnated bronze, the bushings are soft enough not to damage the hard steel spindle in case of an AMB failure. Rubber O–rings are squeezed between the bronze bushings and the steel test housing to provide required stiffness and dampening. One of the auxiliary bushings is only for radial support, and the other bushing performs both radial and axial support. A thin coating, 0.013mm (0.0005in), of Dicronite™applied to the contacting surfaces of the auxiliary bushings provides a smooth surface for the spindle to spin down. The auxiliary bushings were designed to allow orbits of 50% of the nominal clearance in the AMBs.

Compressor

The single stage, unshrouded centrifugal compressor, provided by Kobe Steel, will use both vaned and vaneless diffuser plates. Requiring approximately 55kW gas power, the compressor is designed with an inlet flow rate of 2500m^3/h(1450cfm) and a pressure ratio of 1.7. Drilled and tapped into the compressor housing are twenty Kulite silicon–on–silicon miniature pressure transducers. Each pressure sensor can measure static and dynamic forces. As seen in Figure 7, one sensor is placed in the throat of the compressor, two are along the meridian surface, one is in the diffuser plate, and one sensor is in the volute. This five sensor pattern is then repeated at four different locations around the compressor. This arrangement of sensors enables the capture of stall cells and visualization of surge effects in the compressor.

Both vaned and vaneless diffuser plates will be studied in this compressor with different surge characteristics. The surge control method presented by Sanadgol et al.[6] in a companion paper will investigate the use of both diffusers.

DATA ACQUISITION

Magnetic Bearing Controller

A Linux-based control program using standard state space models was developed, to close the control loop on the magnetic bearing systems. Input signals are captured with Computer Board's CIO-DAS1402/16, 16 bit, 100kHz A/D card. Output is produced by Computer Board's CIO-DAC16/12, 12bit, 16 channel, D/A card. Operating at 10kHz, low-level C programming in Linux performs all the communication between input and output cards. For safety reasons, serial communication provides the ability to remotely access controller parameters via a master computer located 30m(100ft) away.

Data Acquisition

Major data acquisition is performed using LabView™. Two high speed data acquisition (DAQ) cards, National Instruments PXI-6052 and PXI-6071, are used in conjunction with NI's signal processing cards. The Kulite pressure transducers are measured using NI's SCXI-1520 which incorporates a full-bridge with internal 0-10V excitation. Numerous T-type thermocouples are measured with NI's SCXI-1102 which features an internal 2 Hz low pass filter. Where possible, instrumentation is installed in accordance with the 1997 version of the Power Test Code (PTC). Proper sampling rates were set for each instrument to capture all relevant information. Pressure sensors are sampled at 5kHz, position sensors at 3kHz, thermocouples at 10Hz.

FORCE MEASUREMENTS

The method of calculating forces is very important to this research since it is essential to capture accurate force estimates from the AMBs. There are two main methods of measuring force in AMBs. One method uses the amplifier current measurements and position sensor measurements to estimate force with a function, $F = f(i, g)$, where i is the amplifier current and g is the measured air gap. The other method uses Hall effect sensors to measure magnetic flux directly on the pole faces and estimate force by integrating Maxwell's Stress Tensor, $F = \frac{B^2 A_g}{\mu_o}$, where B is the magnetic flux density measured by the Hall effect sensor, A_g is the cross-sectional area of the air gap, and μ_o is the permeability of free space.

Direct measurement of flux though Hall effect sensors gives potentially better accuracy of force measurements but has several limitations. Very thin flux sensors, roughly 0.13mm(0.005in), are extremely expensive. To purchase a flux sensor for each of 12 poles for our radial AMB, along with the DAQ equipment to record the data, would be cost prohibitive at roughly $10,000 per bearing. Thicker flux sensors, roughly 1.0mm(0.040in), are much cheaper but require increasing the air gap to allow proper clearance for the sensor on the pole face. Increasing the air gap causes a drop in the maximum load capacity of the bearings and an increase in required amplifier currents (increased heat). An analysis of our radial AMBs with 1.0mm(0.040in) flux sensors shaved down to 0.50mm(0.020in) thickness showed an unsatisfactory decrease in load capacity. The force capacity of the AMB decreased to roughly half of the load capacity with the original air gap while also requiring active cooling of the windings to compensate for the increased amplifier currents.

Measuring the amplifier currents and spindle position is another method for estimating force loads. The main benefit of this method is that no extra hardware is needed. The position sensors are already needed for the control of the AMBs and the amplifier currents are easily captured. A very simple first order calibration model:

$$F = k_i i + k_g g \tag{1}$$

is commonly used. Unfortunately this force estimation method may introduce significant error because eddy currents, hysteresis and magnetic leakage are not considered. The direct flux method has the benefit of inherently taking these phenomena into account.

Research by Nordmann and Aenis[4] compared both methods of force estimation for a radial bearing. A first order current/position force estimation (1) was compared to the direct flux measurement method of force estimation. Nordmann and Aenis showed that the current/position method produced force accuracies of $\pm$10%FS. The Hall sensor method performed better at $\pm$1%FS. Limiting the operation loading range and position orbits will improve force accuracy. Decreasing the loading range of Nordmann's bearing to 75%FS will reduce the current/position method's predictive uncertainty to $\pm$5% for a centered rotor.

Work by Baun et al.[9] showed that, by using more complex current/position equations and limiting the operating range of the bearing, much better force accuracies can be achieved. A RMS force uncertainty of $\pm$0.76N(0.17lbf), which is $\pm$1.2% for the calibration range $\pm$62N(14lbf), was recorded for a radial AMB. The orbiting range of the bearing was limited to 50% of the nominal air gap and the force load was limited to 75% of the maximum load capacity. The coupled set of calibration equations

$$F = k_e \mathbf{I}^\top \mathbf{N}^\top \mathbf{R}^{-\top}(g, b_e) \mathbf{A}_x \mathbf{R}^{-1}(g, b_e) \mathbf{N} \mathbf{I} \tag{2}$$

was used to estimate the bearing forces. Constants k_e and b_e are the experimental bearing stiffness and bearing reluctance found through calibration.

In (2), **I** is the actuator coil current matrix, **N** is the wire turns matrix, **R** is the reluctance matrix which is a function of gap, g, and b_e and **A** is the pole area matrix. The constants k_e and b_e are found with a gradient based optimization search method[9].

For force estimates of the thrust AMB, Baun used a simpler calibration equation

$$F = k_e \left[\frac{i_1^2}{(2g_1 + b_e)^2} - \frac{i_2^2}{(2g_2 + b_e)^2} \right] \tag{3}$$

Opposing coil currents are i_1 and i_2, while the opposing air gaps are g_1 and g_2. As with (2), the calibration constants k_e and b_e are found with a gradient based optimization search method to minimize the RMS force error between calculated forces and experimentally measured forces. Through careful calibration of the thrust AMB,

a RMS force uncertainty of $\pm$2.3N(0.52lbf), which is $\pm$0.75% of the $\pm$310N(70lbf) calibration range, resulted while limiting the axial displacement to 50% of the nominal air gap.

Using the same force estimation method as Baun with limiting the air gap to 50% of nominal gap and load capacity to 75% of the maximum capacity, we expect to achieve force uncertainties of $\pm$1.2%(12N) for the radial AMB. For the thrust bearing, force uncertainties of $\pm$0.75%(40N) should be achieved. We expect that with further calibration of the bearing over a smaller operating range, better force accuracies can be achieved.

In the end, the limiting source of uncertainty in a magnetic actuator is hysteresis. If uncertainty bounds are based on the major hysteresis loop (as in [4]) then the resulting base uncertainty may be unnecessarily large: careful attention to actuator de–gaussing at a given operating point can take advantage of much smaller local hysteresis loops to reduce force uncertainty substantially. Work presently underway based on the Jiles-Atherton model [10] intends to determine the extent to which such an approach can mitigate the hysteretic uncertainty when the test regimen is comprised of repetitive orbits or fixed points.

SUMMARY

This paper presents several important design specifications for a centrifugal compressor test facility. Explanation of the design placed emphasis on the more practical aspects. All the major components of the test system are described along with design criteria. Testing of the compressor at off-design conditions will help develop analytical tools for future compressor design. Performance estimates are provided where available for various components of the testing system. Finally, the force measurements of the magnetic bearings are analyzed along with an explanation of the force measurement method used.

ACKNOWLEDGEMENTS

The authors would like to thank Toshikazu Miyaji and Koichiro Iizuka from Kobe Steel, LTD for their help in providing the compressor and also SFK Revolve for providing the drive unit for this test facility. Finally, thanks to Lei Zhu for analyzing the performance of the thrust bearing.

REFERENCES

[1] Knopf E. and Nordmann R., 1998, “Active Magnetic Bearings for the Identification of Dynamic Characteristics of Fluid Bearings”,Sixth International Symposium on Magnetic Bearings, *Cambridge, USA, 52-61*

[2] Guinzburg A. and Buse F.W., 1994, “Axial and Radial Forces on a Pump Impeller Obtained with Magnetic-Bearing Force Measurement Rig”, Fourth International Symposium on Magnetic Bearings, *Zurich, Switzerland, 537-542*

[3] Baun D.O. and Flack R.D., 1997, “A Plexiglas Research Pump With Calibrated Magnetic Bearings/LoadCells for Radial and Axial Hydraulic Force Measurements”, ASME Fluids Engineering Division Summer Meeting.

[4] Aenis M. and Nordmann R., 1999, “A Precise Force Measurement in Magnetic Bearings for Diagnosis Purposes”, Proceedings of the Fifth International Symposium on Magnetic Bearings, *NASA Langley, USA, 397-409*.

[5] Spakovsky Z.S., Paduano J.D., Larsonneur R. and Traxler A.,Bright M.M., 2000, “Tip Clearance Actuation with Magnetic Bearing for High Speed Compressor Stall Control”, Proceedings of the ASME Turbo Expo, *Munich, Germany*.

[6] Sanadgol D. and Maslen E.H., 2004, “Sliding Mode Controller for Active Control of Surge in Centrifugal Compressors with Magnetic Thrust Bearing Actuation”, Proceedings of the Ninth International Symposium on Magnetic Bearings, *Lexington, USA*.

[7] Zhu L., Knospe C. and Maslen E., 2004, “Frequency Domain Modeling of Non-laminated Cylindrical Magnetic Actuators”, Proceedings of the Ninth International Symposium on Magnetic Bearings, *Lexington, USA*.

[8] Zhu L., Knospe C. and Maslen E., 2004, “Frequency Domain Modeling of Non-laminated C-shaped Magnetic Actuators”, Proceedings of the Ninth International Symposium on Magnetic Bearings, *Lexington, USA*.

[9] Baun D., 2002, “Hydrodynamic Forces in Centrifugal Pumps and Compressor Impellers in Volute Casings: Measurements using Magnetic Bearings and CFD Simulations”, Ph.D. dissertation, University of Virginia, *Charlottesville, USA*.

[10] Jiles D. and Atherton D., 1986, “Theory of Ferromagnetic Hysteresis”, Journal of Magnetism and Magnetic Materials, *North-Holland, Amsterdam, 48-60*.